

## Appendix A

### Monte Carlo Simulation Details

*These appendices refer to the Monte Carlo simulations and analytic theory which we presented in detail in Ref. [66]. Familiarity with that reference is assumed throughout this discussion.*

In this first Appendix, let me describe some aspects of the Monte Carlo (MC) simulations that lurk behind the scenes, and are not often presented in the light of day. These notes are intended for people wishing to develop MC simulations of their own, or even hoping to debunk our hard-earned and rigorously established results.

#### A.1 Choice of Parameters and Failure Modes

The Monte Carlo (MC) simulations are extremely useful for simulating various experiments, but they can also be very dangerous if the user puts his/her blind faith in their results. We have found that the best approach to the simulations is to treat them like the experiments themselves, and to subject them to intense scrutiny and modeling in order to understand (and, only then, believe) the results. Here I will talk about some failure modes of the simulations that we have studied.

In Ref. [66] we described the simulation in some detail. In that discussion we talked about the probability for two particles, labeled  $k$  and  $l$  to collide. This

probability was said to be given by

$$\tilde{p}_{\text{coll}} = \frac{\sigma_{kl} |\vec{v}_k - \vec{v}_l| \Delta t}{\mathcal{V}_c} . \quad (\text{A.1})$$

Although we said it, and you believed it, this is only true assuming  $\tilde{p}_{\text{coll}}$  is very small. To see why, note that the equilibrium distribution of relative speeds is Gaussian. This means that for any fixed values of cross-section, time-step, and collision volume  $\mathcal{V}_c$ , there is still some finite probability that the relative collision speed will be large enough to make  $\tilde{p}_{\text{coll}}$  greater than one. We conclude that  $\tilde{p}_{\text{coll}}$  does not represent a probability in the conventional sense. The real distribution of times between collisions is given by a Poisson distribution [138], so that the collision probability is

$$\begin{aligned} P_{\text{coll}} &= 1 - \exp(-\tilde{p}_{\text{coll}}) \\ &\simeq \tilde{p}_{\text{coll}} . \end{aligned} \quad (\text{A.2})$$

This is the basis for our statement that  $\langle \tilde{p}_{\text{coll}} \rangle$  should be kept well below  $\sim 10\%$  for accurate results. Note that Eq.(A.2) is still only approximate, as it ignores any possibility for 3-body collisions, or multiple 2-body collisions within a single time-step, but we will see that it is still very good until exceedingly bad choices of the parameters  $\Delta t$  and  $r_c$  are made.

In Fig. A.1 we show the number of collisions per calculated collision time  $\tau_{\text{coll}} = \langle \Gamma_{\text{coll}} \rangle^{-1}$  as a function of  $\langle \tilde{p}_{\text{coll}} \rangle$  for a single-species simulation of particles in equilibrium. When  $\langle \tilde{p}_{\text{coll}} \rangle$  becomes too large, we observe too *few* collisions, since we look for them only once per time-step. The results in Fig. A.1 suggest that the approximation in Eq.(A.2) is still good for  $\langle \tilde{p}_{\text{coll}} \rangle \sim 1$ . Our simulations, which typically use  $\langle \tilde{p}_{\text{coll}} \rangle$  in the range of  $10^{-3}$  to  $10^{-2}$ , are therefore expected to be accurate in this respect.

The other input parameter we use is the critical distance  $r_c$  between atoms. Particles in the simulation must come within  $r_c$  of each other for a collision to be

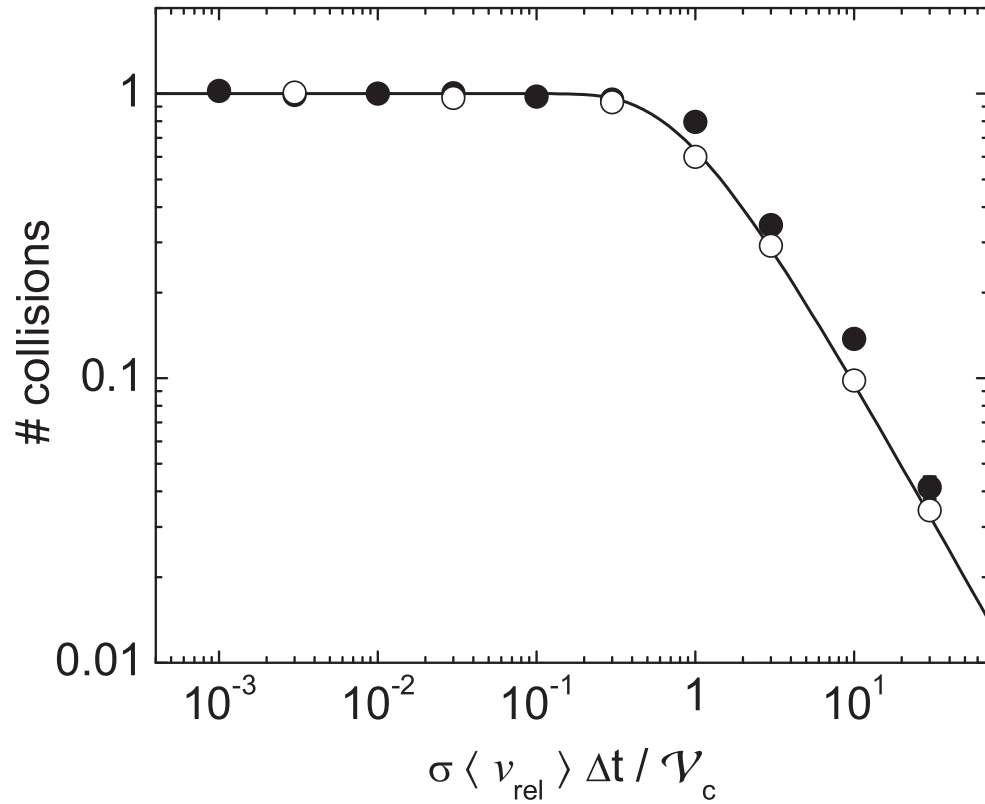


Figure A.1: Effect of bad choice of time-step on the MC simulation. Shown is the number of collisions per calculated collision time as a function of  $\langle \tilde{p}_{\text{coll}} \rangle$  for a single-species gas in equilibrium. Filled points ( $\bullet$ ) use  $\tilde{p}_{\text{coll}}$  and open points ( $\circ$ ) use  $1 - \exp(-\tilde{p}_{\text{coll}})$  to calculate the collision probability in the simulations. The solid line is just the expected behavior for a Poisson distribution. All simulations used  $10^3$  particles with an average of  $10^{-2}$  particles per volume  $\mathcal{V}_c$ .

considered. Although in Ref. [66] we referred to the probability of a cell of volume  $\mathcal{V}_c = 4\pi r_c^3/3$  being occupied, this is again not a probability in the conventional sense, as nothing forbids a choice of parameters where the average number of particles per cell volume  $\mathcal{V}_c$  is greater than 1. Results from the MC simulations are shown in Fig. A.2. If  $\mathcal{V}_c$  is large enough, any given particle will see all  $N - 1$  of the other particles within the volume. The number of collisions per particle in one collision time will then saturate at  $(N - 1) \langle \tilde{p}_{\text{coll}} \rangle$ , since the calculated collision probability is independent of the positions of the particles. Since we are considering dilute gases, one may expect that in the limit  $\mathcal{V}_c \rightarrow 0$  there will be no chance for collisions in the simulations, but this is not the case. If the quantity  $\tilde{p}_{\text{coll}}$  is kept constant, then the time-step  $\Delta t \propto \mathcal{V}_c$ . This means that for every decrease in  $\mathcal{V}_c$ , there must be a corresponding increase in the number of times collisions are searched for. This ensures that a constant rate of collisions is maintained. We again conclude that our insistence on keeping  $\langle n \rangle \mathcal{V}_c$  around  $10^{-3}$  to  $10^{-2}$  is extremely conservative, and should lead to accurate simulations.

## A.2 Transition to Hydrodynamic Behavior

In this section I will use the MC simulations to consider the onset of hydrodynamic behavior in cross-dimensional relaxation (CDR) experiments. Hydrodynamic behavior is generally characterized by a density (or cross-section) so high that a particle undergoes many collisions within a time equal to the trap period. If this happens, the kinetic energy is continuously being re-randomized and the atoms no longer undergo simple harmonic motion in the trap. If one imagines that we begin the CDR experiment with anisotropic energy  $\Omega = E_{x,y}/E_z$ , then collisions will randomize the relative kinetic energies of colliding atoms before they have had a chance to move very far. The gas will then have isotropic kinetic energy, but the potential (and center-of-mass kinetic) energies will still maintain the

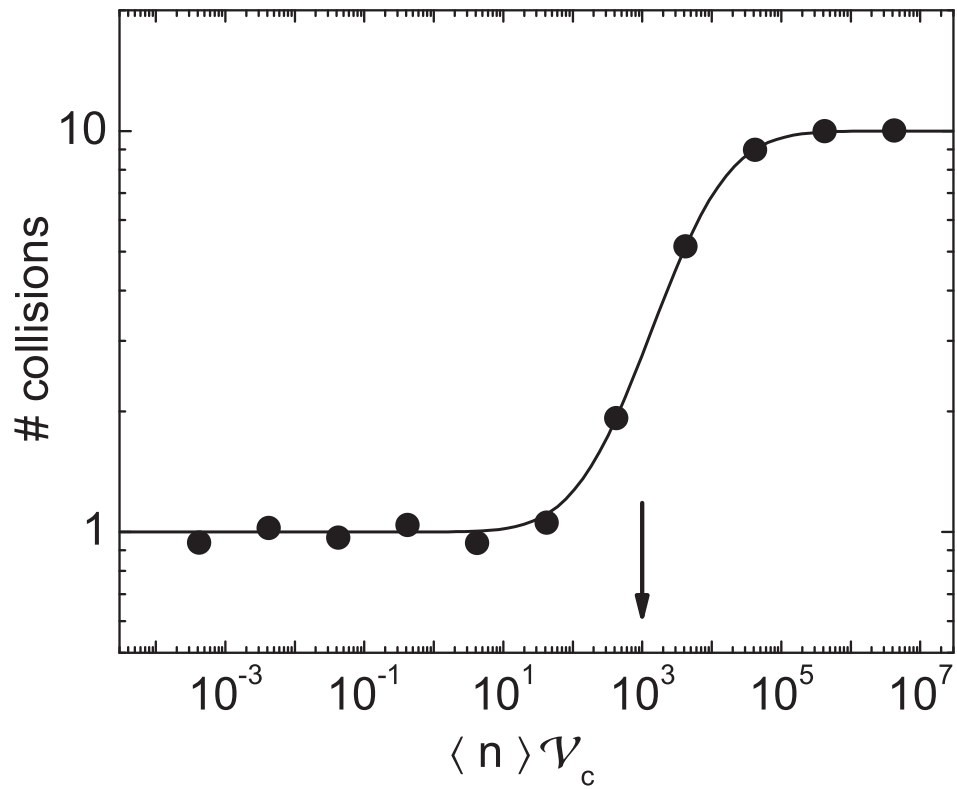


Figure A.2: Effect of bad choice of critical distance of approach on the MC simulation. Shown is the number of collisions per calculated collision time as a function of increasing  $\mathcal{V}_c$  for a single-species gas in equilibrium. The curve is just to guide the eye. All simulations used  $10^3$  particles with  $\langle \tilde{p}_{\text{coll}} \rangle = 10^{-2}$ . The arrow indicates the point where  $\langle n \rangle \mathcal{V}_c = N$ .

initial anisotropy  $\Omega$ . The observed relaxation rate will therefore be slower than in a system with the same collision rate but much higher trapping frequencies.

Our MC simulations typically use atom numbers  $\sim 10^4$  to save computation time. These numbers, however, are expected to leave our simulations in the collisionless regime. To determine when a system like ours enters the hydrodynamic regime I ran a series of simulations of  $^{87}\text{Rb}$ - $^{40}\text{K}$  relaxation with the trapping frequencies fixed to our experimental conditions. The collision rates were varied by either increasing the number of particles, decreasing the temperature (the simulations always use Maxwell-Boltzmann statistics), or increasing the collision cross-sections (with the ratio  $\sigma_{bb}/\sigma_{bf}$  fixed). Results are shown in Fig. A.3. For these simulations, hydrodynamic behavior was observed to begin for  $\langle \Gamma_{\text{coll}} \rangle \sim \omega_{z,\text{K}}$ .

The inset to Fig. A.3 describes the oscillatory behavior which is observed for simulations of CDR in the hydrodynamic regime. An example of the relaxation in this regime is shown in Fig. A.4. Note the  $180^\circ$  phase-shift between oscillations of the axial and radial energies, which means the cloud aspect ratio also oscillates. As the gas goes more deeply into the hydrodynamic regime, the oscillation frequency appears to approach twice the  $^{87}\text{Rb}$  axial frequency. The  $^{87}\text{Rb}$  axial frequency is the lowest trap frequency in the system, and twice this frequency is the frequency at which kinetic and potential energy are exchanged in the absence of collisions. This oscillatory behavior and the nonlinear dependence of the damping rate on the boson density may be used as a guide in experiments. One should be able to clearly identify whether measurements are performed in the collisionless or hydrodynamic regime.

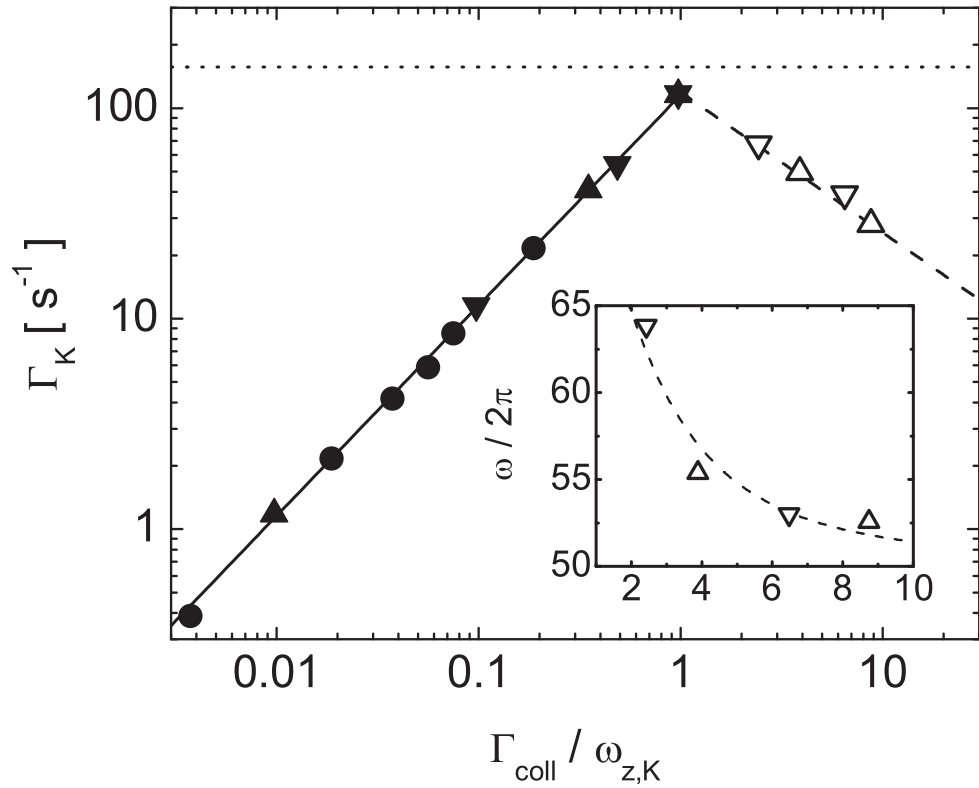


Figure A.3: Nonlinear relaxation rate for CDR due to hydrodynamic effects. Points are from the MC simulations with dots ( $\bullet$ ) varying the number of atoms, up-triangles ( $\blacktriangle$ ) varying the cross-section (with  $|a_{bf}/a_{bb}| = 3$  fixed), and down-triangles ( $\blacktriangledown$ ) varying the temperature. All points used  $N_{\text{Rb}} = 4 N_{\text{K}}$ . The solid line is the collisionless prediction assuming  $\beta = 2.0$  for  $x \leq 1$ , and the dashed line shows a  $x^{-2/3}$  decay for  $x > 1$ , to guide the eye. The dotted line shows the  $^{87}\text{Rb}$  axial trap frequency (in rad/s), which is the lowest trap frequency in the system. Relaxation curves corresponding to the open points ( $\Delta, \nabla$ ) showed hydrodynamic behavior (see Fig. A.4). Damping rates for these simulations were determined from fits to  $E_z(t)$  using damped sines, and neglecting early times. The inset shows the frequency of the hydrodynamic oscillations. For comparison, the dashed curve interpolates between twice the  $^{87}\text{Rb}$  and  $^{40}\text{K}$  axial frequencies ( $2 \times 25$  Hz and  $2 \times 37$  Hz, respectively).

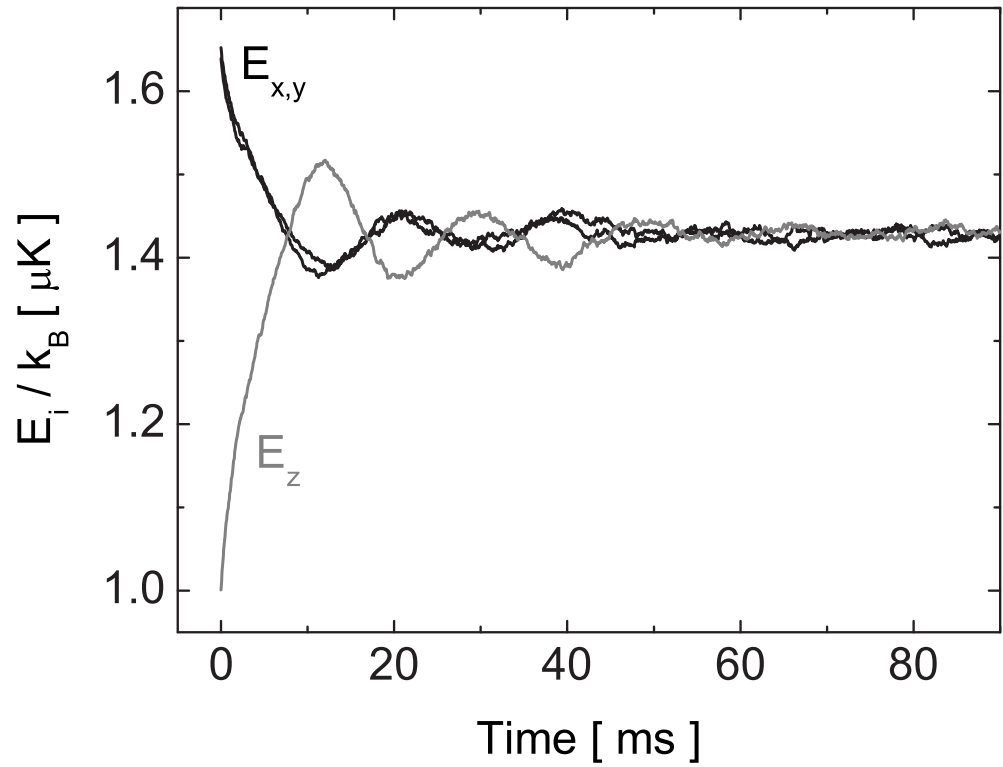


Figure A.4: Signature of hydrodynamic effects on relaxation. Shown is the mean energy per fermion in each direction as a function of time. These curves were taken with  $\langle \Gamma_{\text{coll}} \rangle = 3.9 \omega_z$  for  $^{40}\text{K}$ .